

Massive Vector Form Factors to Three Loops

Matteo Fael^{1,*}, Fabian Lange^{1,2,†}, Kay Schönwald^{1,‡} and Matthias Steinhauser^{1,§}

¹*Institut für Theoretische Teilchenphysik, Karlsruhe Institute of Technology (KIT), 76128 Karlsruhe, Germany*

²*Institut für Astroteilchenphysik, Karlsruhe Institute of Technology (KIT), 76344 Eggenstein-Leopoldshafen, Germany*



(Received 17 February 2022; accepted 30 March 2022; published 29 April 2022)

We compute the three-loop nonsinglet corrections to the photon-quark form factors taking into account the full dependence on the virtuality of the photon and the quark mass. We combine the method of differential equations in an effective way with expansions around regular and singular points. This allows us to obtain results for the form factors with an accuracy of about eight to twelve digits in the whole kinematic range.

DOI: 10.1103/PhysRevLett.128.172003

Introduction.—Form factors are fundamental objects in quantum chromodynamics (QCD) with a variety of applications. On the one hand, they are the simplest objects which show a nontrivial infrared structure and thus form factors are often used to develop and test all-order theorems about the infrared singularities of scattering amplitudes in QCD (see, e.g., Refs. [1–3]). On the other hand, form factors play a crucial role as building blocks in a number of observables which range from low energies to cross sections at the Large Hadron Collider (LHC) at CERN. They describe the universal structure of the $(Z^*, \gamma^*) \rightarrow \bar{Q}Q$ vertex function, involving two on-shell quarks Q and vector or axial-vector couplings of the vector bosons. Massive form factors enter several processes involving heavy quarks at hadron and e^+e^- colliders, such as $\bar{t}t$ production [4–6] and gauge and Higgs boson decays [7–9], which clearly require the inclusion of mass effects. Such processes can probe deviations of the quark couplings from their values in the standard model. Form factors contribute to the all-virtual corrections to cross sections.

In quantum electrodynamics lepton masses are often kept to regulate collinear singularities. Therefore massive form factors take part also in the differential cross section of low-energy lepton scatterings as for instance the elastic $e-p$ scattering [10,11], one of the main avenues for proton radius measurements [12,13], or the $\mu-e$ scattering [11,14], a process able to determine the leading hadronic contribution to the muon anomalous magnetic moment [15–18].

For massless quarks three-loop corrections to the photon-quark form factor have been computed more than ten years ago [19] (see also Refs. [20–23]) and only very

recently the complete four loop results became available [24,25]. Massive quark form factors are known at two-loop order from Refs. [26–33]. At three loops only partial results are available, namely all planar contributions needed for the large- N_c limit (where N_c is the number of colors in QCD) [30,34,35] and the fermionic contributions with closed massless quark loops [33]. For the contribution involving massive closed fermion loops a deep expansion with at least 2000 terms around the on-shell photon limit has been computed in Ref. [36]. Predictions for the high-energy limit at four-loop order are known from Refs. [31,37].

The available results show an involved analytic structure containing iterated integrals with the letters x , $1-x$, $1+x$, and $x - e^{i\pi/3}$, where the relation between x and the photon virtuality $s = q^2$ is given by

$$\frac{q^2}{m^2} = -\frac{(1-x)^2}{x}, \quad (1)$$

with m the mass of the heavy quark. A numerical evaluation of the analytic expressions is possible using, e.g., `ginac` [38,39]. However, depending on the phase space point it might be time consuming and/or its numerical accuracy is limited to a few digits only. Thus, in practice, one often resolves to the construction of approximations which enable a fast numerical evaluation. Moreover, the three-loop results for the color structures which are not yet available in analytic form cannot be expressed in terms of simple iterated integrals. Rather, so-called elliptic integrals are present as the fundamental building blocks. Currently there is no ready-to-use approach for the numerical evaluation of the corresponding mathematical functions and thus especially here numerical approximations are needed.

In this Letter, we present results for the three-loop form factor with an external vector current. We consider QCD with one massive and n_l massless flavors and compute the nonsinglet contribution, where the external quarks directly

Published by the American Physical Society under the terms of the [Creative Commons Attribution 4.0 International license](https://creativecommons.org/licenses/by/4.0/). Further distribution of this work must maintain attribution to the author(s) and the published article's title, journal citation, and DOI. Funded by SCOAP³.

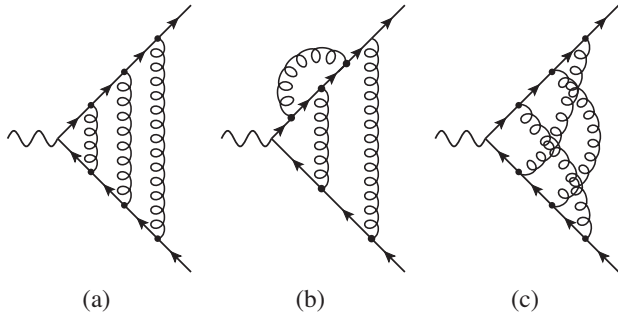


FIG. 1. Sample Feynman diagrams for the vector form factors at three loops. Solid and curly lines denote quarks and gluons, respectively. The external photon is represented by a wavy line.

couple to the current, see also the sample Feynman diagrams in Fig. 1. We perform the reduction to master integrals and establish the differential equations for the latter. They are used in order to construct expansions around singular and regular points using analytic results at $s = 0$ as initial condition. In our calculation we keep the symbols for the Casimir operators of $SU(N_c)$ and thus obtain results for each individual color factor.

There are other methods which are based on difference or differential equations accompanied by expansions [40–47]. Some of them have only been applied to individual master integrals and they are still lacking the proof that they can handle complicated physical problems with a few hundred master integrals. A nontrivial application of Ref. [45] can be found in Ref. [48] where two-loop mixed QCD-electroweak corrections to the associated production of a Higgs boson and a gluon have been computed. In this Letter, we apply the method of Ref. [49] to a nontrivial physical quantity and show that numerically precise results can be obtained in the whole parameter space.

Calculation.—We consider the photon-quark vertex and define the Dirac and Pauli form factors as

$$\Gamma_\mu(q_1, q_2) = F_1(q^2)\gamma_\mu - \frac{i}{2m}F_2(q^2)\sigma_{\mu\nu}q^\nu, \quad (2)$$

with incoming momentum q_1 , outgoing momentum q_2 , and $q = q_1 - q_2$. The external quarks are on-shell and we have $\sigma^{\mu\nu} = i[\gamma^\mu, \gamma^\nu]/2$. The color factor is a simple Kronecker delta in the fundamental color indices of the external quarks and it is suppressed for convenience. F_1 and F_2 can easily be obtained by applying appropriate projectors.

Sample Feynman diagrams are shown in Fig. 1. We generate the amplitudes with `qgraf` [50] and use `q2e` and `exp` [51–53] to rewrite the output to FORM [54] notation and map each diagram to a predefined integral family. In this way we can express F_1 and F_2 as a linear combination of scalar functions with twelve indices where nine correspond to the exponents of propagators and the remaining three to the exponents of irreducible numerators.

For each integral family we use `Kira` [55,56] with `Fermat` [57] to reduce the scalar functions to master integrals. In this step we take care to choose a good basis such that for each entry in our integral tables the dependence on the space-time dimension $d = 4 - 2\epsilon$ and the kinematic variables s and m^2 factorizes in the denominators [58,59]. This is done with the help of an improved version of the program developed in Ref. [58]. `Kira` is also used to minimize the number of master integrals over all 34 families. This allows us to express F_1 and F_2 in terms of 422 master integrals.

In a next step we establish differential equations for the master integrals using `LiteRed` [60,61] and `Kira` and use the results for $s \rightarrow 0$ as initial conditions. In fact, the construction of the solution can be organized such that the naive limit $s = 0$ of a subset of the 422 master integrals is sufficient to fix all unknown constants.

In the limit $s = 0$ the vertex integrals reduce to two-point on-shell integrals, which have been studied in Refs. [62,63]. We use the results for the corresponding master integrals from Ref. [20] which are available up to weight 7. Because of spurious poles in ϵ some of the on-shell master integrals are needed to higher weight which can be constructed with the help of Ref. [64] and PSLQ [65] (see also Ref. [36]). For the current calculation a subset of integrals was needed up to weight 9.

After fixing the initial conditions we can use the differential equations to obtain for each master integral an expansion in s/m^2 up to $(s/m^2)^{75}$. For all other expansions described below we have computed 50 expansion terms. The expansions are constructed by inserting a suitable ansatz into the differential equations and solving the resulting linear system of equations in terms of a small set of boundary conditions. In this context the use of finite fields with a special version of `Kira` and `FireFly` [66,67] was essential for our calculation. Starting from $s = 0$ we move both to negative and positive values of s . To do so we choose values $s_0/m^2 = 1$ and $s_0/m^2 = -4$ and construct generic expansions with the help of the differential equations. They are matched to the $s = 0$ expansion by evaluating the latter numerically at $s/m^2 = 1/2$ and $s/m^2 = -2$, respectively. This provides initial conditions for the s_0 expansions. In total we construct expansions around the following 30 values (note that only one expansion for large absolute values of s is necessary to cover the limits $s \rightarrow \pm\infty$):

$$\frac{s_0}{m^2} \in \{-\infty, -32, -28, -24, -16, -12, -8, -4, 0, 1, 2, 5/2, 3, 7/2, 4, 9/2, 5, 6, 7, 8, 10, 12, 14, 15, 16, 17, 19, 22, 28, 40\} \quad (3)$$

and perform the matching step-by-step starting from $s = 0$. In this way we can cover the whole s/m^2 plane. For more

details on the “expansion and matching” method we refer to Ref. [49].

There are several elements of the calculation which require a significant amount of computer resources. Among them is the reduction to master integrals, where the most involved families required around one week of run-time on eight cores, and the solution of the linear systems of equations to construct series expansions, which took roughly two days per regular expansion point on 20 to 40 cores.

At first sight it seems that the variable x introduced in Eq. (1) is the proper variable to perform the expansions, since the characteristic points $s/m^2 = 0, 4, \infty$ correspond to $x = 1, -1, 0$. However, in practice it is more advantageous to work in s/m^2 . This is also connected to the new threshold at $s/m^2 = 16$ which appears for the first time at three loops. It is mapped to $x = 4\sqrt{3} - 7 \approx -0.072$ which limits the radius of convergence of the variable x .

Let us in the following comment on the choice of s_0 in Eq. (3). Some values correspond to a particular kinematic situation: $s/m^2 = 4$ and 16 correspond to the two- and four-particle thresholds and $m^2/s = 0$ to the high energy limit. Furthermore, as mentioned above, we compute the initial conditions for $s = 0$. To guarantee sufficient accuracy over the whole s/m^2 range we have introduced further expansions for positive and negative values of s . In the differential equations we observe further singularities for $s/m^2 \in \{-4, -2, -1, -1/2, 1/2, 1, 2, 3, 16/3\}$. However, they are spurious since the form factors are regular for these values of s . Nevertheless, for some of them we have constructed an expansion of the master integrals.

For all expansions the convergence around a given value s_0 is only guaranteed up to the next singular point in the complex s plane. For example, for $s_0/m^2 = 22$ we have convergence for $16 < s/m^2 < 28$ and for $s_0/m^2 = -4$ for $-12 < s/m^2 < 4$. Note that $s/m^2 = 4, 16$, and ∞ are singular points of the differential equation which require a power-log expansion. Furthermore, for $s/m^2 = 4$ and 16 we have an expansion in $\sqrt{4 - s/m^2}$ and $\sqrt{16 - s/m^2}$, respectively. For all other points simple Taylor expansions are sufficient.

Often the convergence of a series expansion can be enhanced by switching to a different expansion parameter. One powerful method is based on Möbius transformations as has already been discussed in Ref. [44]. Assume we want to expand around the point x_k and there are singular points of the differential equations at x_{k-1} and x_{k+1} with $x_{k-1} < x_k < x_{k+1}$. Naively, the radius of convergence is limited by the distance to the closer singular point. However, the variable transformation

$$y_k = \frac{(x - x_k)(x_{k+1} - x_{k-1})}{(x - x_{k+1})(x_{k-1} - x_k) + (x - x_{k-1})(x_{k+1} - x_k)} \quad (4)$$

maps the points x_{k-1}, x_k, x_{k+1} to $-1, 0, 1$. The reach of the series expansion is therefore extended in the direction of the farthest singularity although the convergence at the boundaries can be quite slow. We find this mapping indispensable when constructing regular series expansions close to singular points.

The form factors F_1 and F_2 develop both ultraviolet and infrared divergences. The former are taken care of by counterterms for the wave functions and mass of the heavy quarks, which we renormalize on shell. Furthermore, the strong coupling constant is renormalized in the modified minimal subtraction ($\overline{\text{MS}}$) scheme. The remaining infrared poles are described by a universal function independent of the external current, the cusp anomalous dimension Γ_{cusp} , which has been computed to three-loop accuracy in Refs. [68,69]. It is used to construct a $\overline{\text{MS}}$ -like Z factor (for details see, e.g., Ref. [70]) such that the combination

$$F_{1,2} = Z F_{1,2}^f \quad (5)$$

leads to the ultraviolet and infrared finite form factors $F_{1,2}^f$. We introduce their perturbative expansion as

$$F_{1,2}^f = \sum_{n \geq 0} F_{1,2}^{f,(n)} \left(\frac{\alpha_s}{\pi} \right)^n, \quad (6)$$

where $F_1^{f,(0)} = 1$ and $F_2^{f,(0)} = 0$. Since Z is expressed in terms of the strong coupling in the effective n_f -flavor theory we have $\alpha_s \equiv \alpha_s^{(n_f)}(\mu)$ in Eq. (6). In the next section we discuss results for $F_1^{f,(3)}$ and $F_2^{f,(3)}$.

Results.—The results from our calculation are expansions around the values s_0 in Eq. (3). Thus, we can define the form factors F_1 and F_2 piecewise by these expansions. We choose for the renormalization scale $\mu^2 = m^2$.

In the following, we concentrate on F_1 and present results for the renormalized and infrared-subtracted form factor. In Fig. 2 we illustrate the results for the three nonfermionic color structures $C_F^3, C_F^2 C_A, C_F C_A^2$, where C_F and C_A are the Casimir operators of the fundamental and the adjoint representation, respectively, and present results

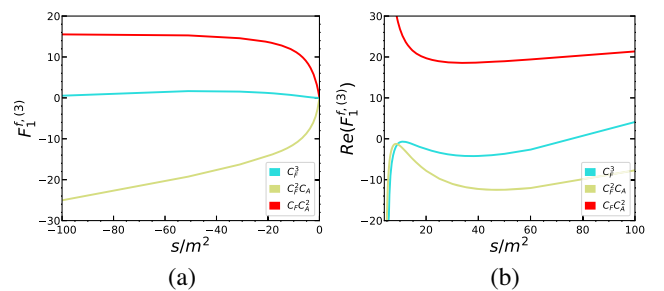


FIG. 2. The color structures $C_F^3, C_F^2 C_A, C_F C_A^2$ of F_1^f as a function of s . We show results for $s < 0$ (a) and $s > 4m^2$ (b).

for $s < 0$ and $s > 4m^2$. For $s = 0$ we have $F_1 = 0$ as can be seen in plot (a). In plot (b) one observes the influence of the Coulomb singularity even for $s/m^2 \approx 10$. The four-particle threshold is much less pronounced. In the high-energy region, both for $s > 0$ and $s < 0$ the form factor contains logarithms up to sixth order.

We estimate the accuracy of our result from the numerical pole cancellations of the renormalized and infrared subtracted form factor. For $s > 4m^2$ the quadratic and linear $1/\epsilon$ poles cancel with a relative precision of 10^{-12} and 10^{-10} , respectively. Assuming a similar progression we estimate that for the finite term we have at least eight significant digits for the coefficients of each color factor. In the regions $0 < s < 4m^2$ and $s < 0$ the accuracy is

significantly higher and in general exceeds twelve significant digits. Also for the fermionic color structures a notably higher accuracy is reached.

In a next step we consider the special kinematic points $s = 0, 4m^2, 16m^2$ and $\pm\infty$ and present (numerical) expansions using the genuine results of our approximation methods. In this Letter we restrict ourselves to the non-fermionic color factors. In the Supplemental Material [71] we present results for the contributions which contain a closed heavy quark loop. The remaining fermionic contributions are available in the literature [33,70].

In the static limit we construct an analytic expansion up to s^{67} from the boundary values at $s = 0$. The first two expansion terms are given by

$$\begin{aligned}
 F_1^{f,(3)}|_{s \rightarrow 0} = & \left\{ C_A C_F^2 \left[\frac{19a_4}{2} - \frac{\pi^2 \zeta_3}{9} + \frac{17725 \zeta_3}{3456} - \frac{55 \zeta_5}{32} + \frac{19l_2^4}{48} - \frac{97}{720} \pi^2 l_2^2 + \frac{29 \pi^2 l_2}{240} - \frac{347 \pi^4}{17280} - \frac{4829 \pi^2}{10368} + \frac{707}{288} \right] \right. \\
 & + C_A^2 C_F \left[-a_4 + \frac{7 \pi^2 \zeta_3}{96} + \frac{4045 \zeta_3}{5184} - \frac{5 \zeta_5}{64} - \frac{l_2^4}{24} + \frac{67}{360} \pi^2 l_2^2 - \frac{5131 \pi^2 l_2}{2880} + \frac{67 \pi^4}{8640} + \frac{172285 \pi^2}{186624} - \frac{7876}{2187} \right] \\
 & + C_F^3 \left[-15a_4 - \frac{17 \pi^2 \zeta_3}{24} - \frac{18367 \zeta_3}{1728} + \frac{25 \zeta_5}{8} - \frac{5l_2^4}{8} - \frac{19}{40} \pi^2 l_2^2 + \frac{4957 \pi^2 l_2}{720} + \frac{3037 \pi^4}{25920} - \frac{24463 \pi^2}{7776} + \frac{13135}{20736} \right] \left. \right\} \frac{s}{m^2} \\
 & + \mathcal{O}\left(\frac{s^2}{m^4}\right) + \text{fermionic contributions}, \quad (7)
 \end{aligned}$$

where $l_2 = \log(2)$, $a_4 = \text{Li}_4(1/2)$, and ζ_n is Riemann's zeta function evaluated at n .

The first two terms for the high-energy expansion of the nonfermionic color structures read

$$\begin{aligned}
 F_1^{f,(3)}|_{s \rightarrow \infty} = & 4.7318 C_F^3 - 20.762 C_F^2 C_A + 8.3501 C_F C_A^2 + [3.4586 C_F^3 - 4.0082 C_F^2 C_A - 6.3561 C_F C_A^2] l_s \\
 & + [1.4025 C_F^3 + 0.51078 C_F^2 C_A - 2.2488 C_F C_A^2] l_s^2 + [0.062184 C_F^3 + 0.90267 C_F^2 C_A - 0.42778 C_F C_A^2] l_s^3 \\
 & + [-0.075860 C_F^3 + 0.20814 C_F^2 C_A - 0.035011 C_F C_A^2] l_s^4 + [-0.023438 C_F^3 + 0.019097 C_F^2 C_A] l_s^5 \\
 & + [-0.0026042 C_F^3] l_s^6 - \{-92.918 C_F^3 + 123.65 C_F^2 C_A - 47.821 C_F C_A^2 + [-10.381 C_F^3 + 2.3223 C_F^2 C_A \\
 & + 17.305 C_F C_A^2] l_s + [4.9856 C_F^3 - 19.097 C_F^2 C_A + 8.0183 C_F C_A^2] l_s^2 \\
 & + [3.0499 C_F^3 - 6.8519 C_F^2 C_A + 1.9149 C_F C_A^2] l_s^3 + [0.67172 C_F^3 - 0.91213 C_F^2 C_A \\
 & + 0.24069 C_F C_A^2] l_s^4 + [0.13229 C_F^3 - 0.051389 C_F^2 C_A + 0.0043403 C_F C_A^2] l_s^5 \\
 & + [0.0041667 C_F^3 - 0.0010417 C_F^2 C_A - 0.00052083 C_F C_A^2] l_s^6 \left. \right\} \frac{m^2}{s} + \mathcal{O}\left(\frac{m^4}{s^2}\right) + \text{fermionic contributions}, \quad (8)
 \end{aligned}$$

with $l_s = \log[m^2/(-s - i\delta)]$. The leading logarithmic contributions of the order $\alpha_s^n \log^{2n}(m^2/s)$ are given by the Sudakov exponent [72,73] $\exp[-C_F \alpha_s/(4\pi) \times \log^2(m^2/s)]$ which is reproduced by our expansions. In fact, in our calculation we can even reconstruct the analytic results of the coefficients which are given by

$$F_1^{f,(3)} = -\frac{C_F^3}{384} l_s^6 - \frac{m^2}{s} \left(\frac{C_F^3}{240} - \frac{C_F^2 C_A}{960} - \frac{C_F C_A^2}{1920} \right) l_s^6 + \dots \quad (9)$$

In Eq. (8) they are shown in numeric form. Note that also the leading logarithms of the mass corrections m^2/s perfectly agree with Ref. [74] where the results in Eq. (9) have been obtained using an involved asymptotic expansion of the three-loop vertex diagrams. Our approach provides the whole tower of logarithms and also higher order m^2/s contributions. We estimate the accuracy of the nonlogarithmic term in Eq. (8) to ten digits. For the subleading terms the accuracy decreases. Note, however,

that we use the $s \rightarrow \infty$ expansion only for $|s/m^2| \gtrsim 45$ and that $1/45^3 \approx \mathcal{O}(10^{-5})$.

Let us next discuss the thresholds at $s = 4m^2$ and $s = 16m^2$. Close to the two-particle threshold F_1 develops the famous Coulomb singularity with negative powers in the velocity of the produced quarks, $\beta = \sqrt{1 - 4m^2/s}$, up to third order multiplied by $\log(\beta)$ terms. Close to threshold it is interesting to consider the combination of F_1 and F_2

$$\frac{3}{2}\Delta = |F_1 + F_2|^2 + \frac{|(1 - \beta^2)F_1 + F_2|^2}{2(1 - \beta^2)}, \quad (10)$$

which is closely related to the cross section of heavy quark production in electron positron annihilation via $\sigma(e^+e^- \rightarrow Q\bar{Q}) = \sigma_0\beta 3\Delta/2$ with $\sigma_0 = 4\pi\alpha^2 Q_Q^2/(3s)$, where α is the fine structure constant and Q_Q is the fractional charge of the massive quark Q . For $\beta \rightarrow 0$ real radiation is suppressed by two powers of β which allows us to provide the first two terms in the expansion for each color factor. Our result for the third order correction $\Delta^{(3)}$ reads

$$\begin{aligned} \Delta^{(3)} = & C_F^3 \left[-\frac{32.470}{\beta^2} + \frac{1}{\beta} (14.998 - 32.470 l_{2\beta}) \right] \\ & + C_A^2 C_F \frac{1}{\beta} [16.586 l_{2\beta}^2 - 22.572 l_{2\beta} + 42.936] \\ & + C_A C_F^2 \left[\frac{1}{\beta^2} (-29.764 l_{2\beta} - 7.770339) \right. \\ & \left. + \frac{1}{\beta} (-12.516 l_{2\beta} - 11.435) \right] + \mathcal{O}(\beta^0) \\ & + \text{fermionic contributions,} \end{aligned} \quad (11)$$

with $l_{2\beta} = \log(2\beta)$. Our numerical results reproduce the analytic expressions from Ref. [75] (see also Refs. [76,77]) with at least 13 digits accuracy.

Four-particle thresholds are present in diagrams which contain a closed heavy quark loop but also in purely gluonic diagrams like the one in Fig. 1(b). Interestingly it has a smooth behavior. In fact, we observe the first nonanalytic terms at order $(\beta_4)^9$ with $\beta_4 = \sqrt{1 - 16m^2/s}$. Note that the massive four-particle phase-space, which is one of our master integrals, already provides a factor $(\beta_4)^7$. Furthermore, our expansions of F_1 and F_2 up to $(\beta_4)^{50}$ do not contain any $\log \beta_4$ terms although many of the master integrals contain such terms.

Finally, we want to mention that we have performed the calculation for general QCD gauge parameter ξ and have checked that ξ cancels in the renormalized form factors. Note that both the bare three-loop expressions and the quark mass counterterm contributions depend on ξ . Furthermore, we can specify our result to the large- N_c limit and compare against the exact results from Ref. [30]. In this limit only about 90 planar master integrals contribute

and we observe a significantly increased precision of our result. In fact, in the whole s/m^2 region we can reproduce the exact result with at least 14 digits.

Conclusions.—In this Letter, we present for the first time results for the nonsinglet three-loop massive photon-quark form factors taking into account all color structures. We use the methods based on “expansion and matching” as introduced in Ref. [49] and obtain numerical approximations in the whole s/m^2 range. Based on the comparison to the partially known exact results and on internal cross checks of the method we estimate the accuracy to at least eight significant digits above the $s = 4m^2$ threshold and to about twelve digits below. Note that, if required, a systematic improvement is possible by adding more intermediate matching points. The application to a physical quantity with a nontrivial analytic structure shows the effectiveness of our method.

We thank Roman Lee for discussions about the Möbius transformations and Alexander Smirnov and Vladimir Smirnov for discussions about the basis change for the master integrals and providing an improved version of the *Mathematica* code from Ref. [58]. This research was supported by the Deutsche Forschungsgemeinschaft (DFG, German Research Foundation) under Grant No. 396021762—TRR 257 “Particle Physics Phenomenology after the Higgs Discovery.” The Feynman diagrams were drawn with the help of Axodraw [78] and JaxoDraw [79].

*matteo.fael@kit.edu

†fabian.lange@kit.edu

‡kay.schoenwald@kit.edu

§matthias.steinhauser@kit.edu

- [1] A. Mitov and S.-O. Moch, *J. High Energy Phys.* **05** (2007) 001.
- [2] T. Becher and M. Neubert, *Phys. Rev. D* **79**, 125004 (2009); **80**, 109901(E) (2009).
- [3] M. Beneke, P. Falgari, and C. Schwinn, *Nucl. Phys.* **B828**, 69 (2010).
- [4] S.-O. Moch and P. Uwer, *Phys. Rev. D* **78**, 034003 (2008).
- [5] N. Kidonakis and R. Vogt, *Phys. Rev. D* **78**, 074005 (2008).
- [6] G. Moortgat-Pick, H. Baer, M. Battaglia, G. Belanger, K. Fujii, J. Kalinowski, S. Heinemeyer, Y. Kiyo, K. Olive, F. Simon *et al.*, *Eur. Phys. J. C* **75**, 371 (2015).
- [7] W. Bernreuther, R. Bonciani, T. Gehrmann, R. Heinesch, P. Mastrolia, and E. Remiddi, *Phys. Rev. D* **72**, 096002 (2005).
- [8] W. Bernreuther, L. Chen, and Z.-G. Si, *J. High Energy Phys.* **07** (2018) 159.
- [9] A. Behring and W. Bizoń, *J. High Energy Phys.* **01** (2020) 189.
- [10] R.-D. Bucoveanu and H. Spiesberger, *Eur. Phys. J. A* **55**, 57 (2019).
- [11] P. Banerjee, T. Engel, A. Signer, and Y. Ulrich, *SciPost Phys.* **9**, 027 (2020).

- [12] J. C. Bernauer, P. Achenbach, C. Ayerbe Gayoso, R. Böhm, D. Bosnar *et al.* (A1 Collaboration), *Phys. Rev. Lett.* **105**, 242001 (2010).
- [13] W. Xiong, A. Gasparian, H. Gao, D. Dutta, M. Khandaker, N. Liyanage, E. Pasyuk, C. Peng, X. Bai, L. Ye *et al.*, *Nature (London)* **575**, 147 (2019).
- [14] C. M. Carloni Calame, M. Chiesa, S. M. Hasan, G. Montagna, O. Nicosini, and F. Piccinini, *J. High Energy Phys.* **11** (2020) 028.
- [15] C. M. Carloni Calame, M. Passera, L. Trentadue, and G. Venanzoni, *Phys. Lett. B* **746**, 325 (2015).
- [16] G. Abbiendi, C. M. Carloni Calame, U. Marconi, C. Matteuzzi, G. Montagna, O. Nicosini, M. Passera, F. Piccinini, R. Tenchini, L. Trentadue *et al.*, *Eur. Phys. J. C* **77**, 139 (2017).
- [17] G. Abbiendi *et al.*, Letter of intent: The MUonE project, Reports No. CERN-SPSC-2019-026, No. SPSC-I-252, 2019.
- [18] P. Banerjee, C. M. Carloni Calame, M. Chiesa, S. Di Vita, T. Engel, M. Fael, S. Laporta, P. Mastrolia, G. Montagna, O. Nicosini *et al.*, *Eur. Phys. J. C* **80**, 591 (2020).
- [19] P. A. Baikov, K. G. Chetyrkin, A. V. Smirnov, V. A. Smirnov, and M. Steinhauser, *Phys. Rev. Lett.* **102**, 212002 (2009).
- [20] R. N. Lee and V. A. Smirnov, *J. High Energy Phys.* **02** (2011) 102.
- [21] T. Gehrmann, E. W. N. Glover, T. Huber, N. Ikizlerli, and C. Studerus, *J. High Energy Phys.* **06** (2010) 094.
- [22] T. Gehrmann, E. W. N. Glover, T. Huber, N. Ikizlerli, and C. Studerus, *J. High Energy Phys.* **11** (2010) 102.
- [23] A. von Manteuffel, E. Panzer, and R. M. Schabinger, *Phys. Rev. D* **93**, 125014 (2016).
- [24] R. N. Lee, A. von Manteuffel, R. M. Schabinger, A. V. Smirnov, V. A. Smirnov, and M. Steinhauser, *Phys. Rev. D* **104**, 074008 (2021).
- [25] R. N. Lee, A. von Manteuffel, R. M. Schabinger, A. V. Smirnov, V. A. Smirnov, and M. Steinhauser, *arXiv*: 2202.04660.
- [26] P. Mastrolia and E. Remiddi, *Nucl. Phys.* **B664**, 341 (2003).
- [27] R. Bonciani, P. Mastrolia, and E. Remiddi, *Nucl. Phys.* **B676**, 399 (2004).
- [28] W. Bernreuther, R. Bonciani, T. Gehrmann, R. Heinesch, T. Leineweber, P. Mastrolia, and E. Remiddi, *Nucl. Phys.* **B706**, 245 (2005).
- [29] J. Gluza, A. Mitov, S. Moch, and T. Riemann, *J. High Energy Phys.* **07** (2009) 001.
- [30] J. Henn, A. V. Smirnov, V. A. Smirnov, and M. Steinhauser, *J. High Energy Phys.* **01** (2017) 074.
- [31] T. Ahmed, J. M. Henn, and M. Steinhauser, *J. High Energy Phys.* **06** (2017) 125.
- [32] J. Ablinger, A. Behring, J. Blümlein, G. Falcioni, A. De Freitas, P. Marquard, N. Rana, and C. Schneider, *Phys. Rev. D* **97**, 094022 (2018).
- [33] R. N. Lee, A. V. Smirnov, V. A. Smirnov, and M. Steinhauser, *J. High Energy Phys.* **03** (2018) 136.
- [34] J. Ablinger, J. Blümlein, P. Marquard, N. Rana, and C. Schneider, *Phys. Lett. B* **782**, 528 (2018).
- [35] J. Ablinger, J. Blümlein, P. Marquard, N. Rana, and C. Schneider, *Nucl. Phys.* **B939**, 253 (2019).
- [36] J. Blümlein, P. Marquard, N. Rana, and C. Schneider, *Nucl. Phys.* **B949**, 114751 (2019).
- [37] J. Blümlein, P. Marquard, and N. Rana, *Phys. Rev. D* **99**, 016013 (2019).
- [38] C. Bauer, A. Frink, and R. Kreckel, *J. Symb. Comput.* **33**, 1 (2002).
- [39] J. Vollinga and S. Weinzierl, *Comput. Phys. Commun.* **167**, 177 (2005).
- [40] S. Laporta, *Int. J. Mod. Phys. A* **15**, 5087 (2000).
- [41] R. Boughezal, M. Czakon, and T. Schutzmeier, *J. High Energy Phys.* **09** (2007) 072.
- [42] J. Blümlein and C. Schneider, *Phys. Lett. B* **771**, 31 (2017).
- [43] X. Liu, Y.-Q. Ma, and C.-Y. Wang, *Phys. Lett. B* **779**, 353 (2018).
- [44] R. N. Lee, A. V. Smirnov, and V. A. Smirnov, *J. High Energy Phys.* **03** (2018) 008.
- [45] F. Moriello, *J. High Energy Phys.* **01** (2020) 150.
- [46] M. Hidding, *Comput. Phys. Commun.* **269**, 108125 (2021).
- [47] I. Dubovyk, A. Freitas, J. Gluza, K. Grzanka, M. Hidding, and J. Usovitsch, *arXiv*:2201.02576.
- [48] M. Becchetti, F. Moriello, and A. Schweitzer, *arXiv*:2112.07578.
- [49] M. Fael, F. Lange, K. Schönwald, and M. Steinhauser, *J. High Energy Phys.* **09** (2021) 152.
- [50] P. Nogueira, *J. Comput. Phys.* **105**, 279 (1993).
- [51] R. Harlander, T. Seidensticker, and M. Steinhauser, *Phys. Lett. B* **426**, 125 (1998).
- [52] T. Seidensticker, *arXiv*:hep-ph/9905298.
- [53] <http://sfb-tr9.ttp.kit.edu/software/html/q2eexp.html>.
- [54] J. Kuipers, T. Ueda, J. A. M. Vermaseren, and J. Vollinga, *Comput. Phys. Commun.* **184**, 1453 (2013).
- [55] P. Maierhöfer, J. Usovitsch, and P. Uwer, *Comput. Phys. Commun.* **230**, 99 (2018).
- [56] J. Klappert, F. Lange, P. Maierhöfer, and J. Usovitsch, *Comput. Phys. Commun.* **266**, 108024 (2021).
- [57] R. H. Lewis, Fermat's user guide, <http://home.bway.net/lewis>.
- [58] A. V. Smirnov and V. A. Smirnov, *Nucl. Phys.* **B960**, 115213 (2020).
- [59] J. Usovitsch, *arXiv*:2002.08173.
- [60] R. N. Lee, *arXiv*:1212.2685.
- [61] R. N. Lee, *J. Phys. Conf. Ser.* **523**, 012059 (2014).
- [62] S. Laporta and E. Remiddi, *Phys. Lett. B* **379**, 283 (1996).
- [63] K. Melnikov and T. van Ritbergen, *Phys. Lett. B* **482**, 99 (2000).
- [64] R. N. Lee and K. T. Mingulov, *Comput. Phys. Commun.* **203**, 255 (2016).
- [65] H. R. P. Ferguson, D. H. Bailey, and S. Arno, *Math. Comput.* **68**, 351 (1999).
- [66] J. Klappert and F. Lange, *Comput. Phys. Commun.* **247**, 106951 (2020).
- [67] J. Klappert, S. Y. Klein, and F. Lange, *Comput. Phys. Commun.* **264**, 107968 (2021).
- [68] A. Grozin, J. M. Henn, G. P. Korchemsky, and P. Marquard, *Phys. Rev. Lett.* **114**, 062006 (2015).
- [69] A. G. Grozin, J. M. Henn, G. P. Korchemsky, and P. Marquard, *J. High Energy Phys.* **01** (2016) 140.
- [70] R. N. Lee, A. V. Smirnov, V. A. Smirnov, and M. Steinhauser, *J. High Energy Phys.* **05** (2018) 187.

- [71] See Supplemental Material at <http://link.aps.org/supplemental/10.1103/PhysRevLett.128.172003> for the results for the form factor F_1 involving a closed heavy quark loop.
- [72] V. V. Sudakov, Sov. Phys. JETP **3**, 65 (1956), <http://jetp.ras.ru/cgi-bin/e/index/e/3/1/p65?a=list>.
- [73] J. Frenkel and J. C. Taylor, Nucl. Phys. **B116**, 185 (1976).
- [74] T. Liu, A. A. Penin, and N. Zerf, Phys. Lett. B **771**, 492 (2017).
- [75] Y. Kiyo, A. Maier, P. Maierhöfer, and P. Marquard, Nucl. Phys. **B823**, 269 (2009).
- [76] A. Pineda and A. Signer, Nucl. Phys. **B762**, 67 (2007).
- [77] A. H. Hoang, V. Mateu, and S. Mohammad Zebarjad, Nucl. Phys. **B813**, 349 (2009).
- [78] J. A. M. Vermaseren, Comput. Phys. Commun. **83**, 45 (1994).
- [79] D. Binosi and L. Theußl, Comput. Phys. Commun. **161**, 76 (2004).